International Conference on Space Optics—ICSO 2022

Dubrovnik, Croatia

3–7 October 2022

Edited by Kyriaki Minoglou, Nikos Karafolas, and Bruno Cugny,

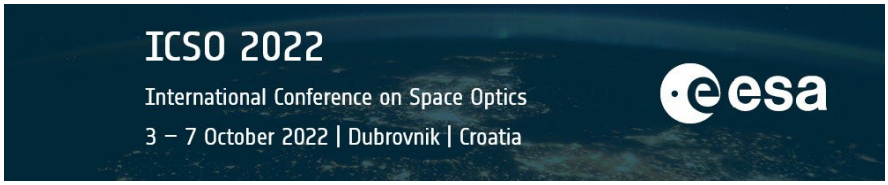

Feasibility study of a Terabit/s GEO-to-Ground WDM Optical Communication Link

International Conference on Space Optics — ICSO 2022, edited by Kyriaki Minoglou, Nikos Karafolas, Bruno Cugny, Proc. of SPIE Vol. 12777, 127776J · © 2023 ESA and CNES · 0277-786X · doi: 10.1117/12.2691132

Feasibility study of a Terabit/s GEO-to-Ground WDM Optical Communication Link

Veronica Spirito[a], Giulio Cossu[a], and Ernesto Ciaramella[a]

[a]Scuola Superiore Sant'Anna, Pisa, ITALY

ABSTRACT

Future space communications will transfer huge volumes of data, especially from space to Earth. To this aim, Free Space Optics (FSO) communications are a unique alternative to Radio Frequency (RF), as they offer much higher data rate and can leverage upon existing fiber communication technology. Here, with a realistic approach, we theoretical asses a new solution at 1.6 Tbit/s, based on a Wavelength Division Multiplexing (WDM) communication system enabled by transparent terminals. We quantify the impact of the atmosphere in terms of terminal size and propagation effects. We derive an accurate power budget in realistic implementation options, considering different system parameters and channel conditions, highlighting practical limitations from the optical technology at the transmitter and receiver side, as well as the possible countermeasures.

1. INTRODUCTION

Today and future space missions are expected to transmit huge volumes of scientific data, including high-definition images and video especially from Space to Earth.[1,2] Moreover, communications and network providers have to face the ever-increasing demands for high capacity from business customers, which are driven by many different applications (e.g., e-commerce, industrial automation, Internet of things (IoT) etc.). This leads to a significant increase of the required bandwidth and the need for new technologies capable of transmitting at much higher data rates than present. However, the licensed Radio Frequency (RF) spectrum is not enough,[1] so that the unique valid alternative is the Free Space Optical Communication (FSOC).

Indeed, both space agencies and private companies invest today hugely in several missions and programs to establish Inter-Satellite-Links (ISLs) and the most challenging Feeder-Links (FLs), passing through the terrestrial atmosphere. Among them, we can cite National Aeronautics and Space Administration (NASA),[3] European Space Agency (ESA),[4,5] Japan Aerospace eXploration Agency (JAXA),[?,6] and SpaceX company.[7,8] To this aim, future FSOCs will take advantage of 50-years R&D in the optical fiber industry, including developments of high-speed photonic components, wavelength-multiplexing, modulation and coding schemes.

In the near future, FSOCs can offer very high data rates, while satisfying the Size Weight and Power consumption (SWaP) constraints. Indeed, at a given transmitter power, the received intensity can be much greater thanks to the much lower beam divergence (proportional to λ/D, where λ is the carrier wavelength and D is the aperture diameter) than in RF communications. On the other hand, this leads to stricter requirements for beam pointing (e.g. around few micro radians), so much that, usually, an accurate Pointing, Acquisition and Tracking (PAT) technique is adopted to satisfy them.[9,10]

However, the performance of a very high data rate FL can be quite limited by the propagation through the atmosphere (e.g., absorption, scattering and, most important, turbulence). As in uplink the channel impairments take place close to the transmitter, while in downlink they take place close to the receiver, this leads to asymmetric impairments of the communication in the two cases.[11]

Today the demand for a very high-capacity downlink is very urgent[1] and this is particularly challenging for the Geostationary (GEO) satellites (typical distance from Earth surface around 36000 km). Thus, we present here the theoretical assessment of the GEO-Earth downlink power budget of a Wavelength Division Multiplexing (WDM) optical communication systems, with a realistic approach. The FSOC system is possible thanks to

Further author information:
Veronica Spirito, E-mail: veronica.spirito@santannapisa.it

a new solution based on transparent terminals described in 2, and leverages upon existing optical fiber communication technology subsystems. We choose 40 wavelength channels in the C-band (1530 nm to 1565 nm), each carrying a 40 Gbit/s On-Off Keying (OOK) signal with a Reed-Solomon (RS) Forward Error Correction (FEC) code. This allows to reach a total aggregated throughput of 1.6 Tbit/s and we will see that the system design can be successfully carried out, provided that a careful design is carried out. We will also determine the conditions under which the system can provide the expected performance.

2. SCENARIO

Despite the great potential of FSOCs, feeder links can suffer from significant drawbacks due to the atmosphere, including attenuation (e.g., different types of clouds), scattering and refractive index fluctuations, which can resulting into fades at the expense of lowers link availability compared with the RF band.

In Fig. 1, we show the typical scenario for feeder links, where an OGS is receiving optical signals from a satellite. For the sake of clarity, uplink and downlink are indicated with two different colors. In downlink, the broadening of the optical beam is mostly due to diffraction, and a minor spread is due to the atmospheric effect or variation in the beam steering. In fact, close to the receiver, the wave can be modelled as a plan wave. The scintillation penalty is in general quite small with respect to the uplink. In the downlink signal, the main contribution for degradation of the signal quality is due to atmospheric losses (related to absorption and scattering), beam spreading due to diffraction effect, and loss of spatial coherence. To mitigate all those impairments affecting the propagating signal some countermeasures might be adopted.[12] The overall scenario parameters are summarized in Table 1.

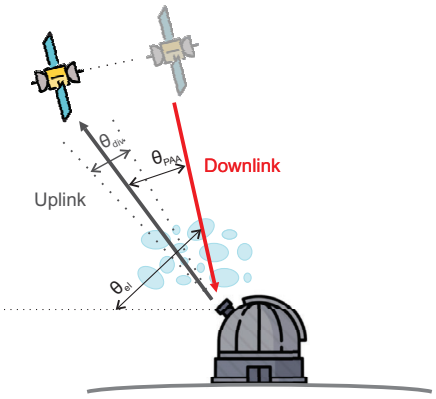

Figure 1: Satellite-ground communication scenario.

Table 1: Summary of scenario parameters for this study.

SCENARIO PARAMETERS	
GEO satellite altitude at zenith [km]	35786
Optical Ground Station (OGS) altitude [m]	2370
Space and ground telescopes optics fixed losses [dB]	3
Point-Ahead Angle (PAA) [µrad]	18
Satellite slew-rate [µrad]	73

In this type of FSOC system, a key role is played by the Adaptive Optics (AO) at the ground station. In fact, in the transparent terminal represented in Figure 2, the received WDM signals must be efficiently coupled into a single mode fiber (SMF). To this aim, the phase distortions due to turbulence have to be removed by the

AO, which corrects the distorted wavefront to increase the coupling efficiency. Then, the signals are amplified by a low noise Erbium-doped Fiber Amplifier (EDFA): due to high losses, the power at the input of this Low Noise Amplifier (LNA) is quite low, which has a direct impact on the Optical Signal to Noise Ratio (OSNR). The system performance is then basically determined by the OSNR value, a regime that we can call OSNR-limited. Then the signals are WDM-demultiplexed and filtered by a common component (Arrayed Waveguide Grating (AWG)). Finally, each wavelength signal is translated to the electrical domain by a common opto-electronic board.

2.1 System simulations

We carried out our system assessment by combining our homemade MATLAB®-based code with results obtained by means of VPI Photonics commercial software. The last is used to determine the received OSNR as function of input power and then the corresponding Bit Error Rate (BER) value (before and after FEC decoding).

The presented estimations are all based on the assumption of a single high-power optical booster EDFA output power amplifying simultaneously all the optical WDM channels, as envisaged by ESA.[13] We performed Monte-Carlo simulations examining different turbulent regimes and atmospheric conditions defined in Table 2.

Based on the technology currently available or to be available in the coming years, the final goal of our analyses is to identify the best trade-off taking into account the cost-complexity and communication performance to give recommendations and constraints for the future design of high data rate space-based optical communication network. Our analysis begins with the design of a system (System A), where we assume existing space and ground terminals characteristics. The most challenging link is for the "stressing atmospheric and meteorological conditions" for the lowest 30° elevation angle. With the intent to close the link budget with a safety margin of 3 dB, we select the best transmitter diameter decreasing its obscuration factor. In fact, if on one side, according to the rule of geometric diffraction, the smaller the initial beam waist, the greater the widening of the beam and therefore the smaller are the losses for pointing; on the other side, if the transmitter diameter is too small, the antenna gain is not enough to compensate for the geometric losses. A trade off must be performed. In the end, we thus propose a slightly different system (System B) changing the transmitter obscuration factor, both the transmitter and receiver aperture diameters, and the effectiveness of the turbulence compensation countermeasures.

It is due to highlight that the PAT subsystem, which works prior to link establishment, is not considered in our model. We assumed a collimated Gaussian beam and the pointing error and turbulence as two independent phenomena.[14] Once the two transceivers have locked onto each other, we assume a 3-sigma total pointing accuracy (around 99.7%) with a residual radial pointing error θ_{point} due to platform mechanical vibrations (in Section 3.3). Moreover, our analyses are performed not exactly at 90 deg of elevation angle, but at 86 deg, because of the well-known nadir singularity of the PAT system through zenith with an azimuth direction at the OGS.[15]

We considered a WDM system with 40 optical signals in the C-band, as illustrated in Fig. 2. Here, we see the various channels, with 100 GHz channel spacing, each externally modulated by a 40 Gbit/s OOK sequence. They are multiplexed by means of an AWG multiplexer, amplified by a single 50 dBm space-qualified booster EDFA, simultaneously amplifying all the optical WDM channels.[13]

Figure 2: Structure of the WDM FSOC system, including (de-)multiplexers, amplifiers (EDFA) and telescopes.

After free-space propagation, the optical wave is collected by a telescope, passes through a AO system and then the signals are pre-amplified by means of an pre-amplifier EDFA, then they are demultiplexed and filtered, and finally detected by an array of PIN photo detectors. Each receiver performs direct detection, followed by clock and data recovery, symbol decision and FEC decoding.

Assuming the aforementioned characteristics summarized in Table 5, we first assess the BER curve (after FEC) as function of input power by a home-made VPI Photonics schematic. We emulate the optical equipment

behaviour in a back-to-back configuration: at any input power, we obtain a reliable estimation of the OSNR, include the effects of all other noise sources, derive the uncorrected BER value and then obtain the BER corrected by the FEC. We thus obtain our back-to-back reference curve.

Then, we use our software to combine this information with a time-varying channel behaviour, including also the residual pointing losses, and the performance of the AO system. We eventually compute the resulting power budget versus the elevation angles considering all the impairments and gains introduced by the applied countermeasures (e.g. atmospheric parameters, channel losses, fiber coupling adopting the AO system). As previously stated, the following analyses were performed assuming a well-established link, i.e., after PAT is perfectly locked.

3. TRANSMISSION IMPAIRMENTS

3.1 Absorption and scattering

Along the atmospheric path, the optical signal experiences an attenuation caused by absorption by suspended molecules, Mie scattering by molecules or aerosol particles, and Rayleigh scattering. In C band, Mie scatter (especially due to fog) is dominant since the scatter site is on the order of the wavelength of light.[16,17] As the optical beam propagates, its attenuation is expressed by the Beer-Lambert law as function of the atmospheric transmittance[17]

$$\frac{I(L)}{I(0)} = e^{-\alpha L} \tag{1}$$

where I(0) is the transmitted laser power at the source and I(L) is the laser power at a distance L, α is the total attenuation factor in km^{-1}, which includes both absorption and scattering. Although small,[17] we also include the absorption contribution. We then express α as:

$$\alpha = \alpha_{abs} + \alpha_{scatt} \tag{2}$$

where α_{abs} and α_{scatt} are the absorption and the scattering contribution, respectively. For the given atmospheric conditions, at the 86° of elevation angle we computed the first input using MODTRAN®. We set the Mid-Latitude Summer model and a rural aerosol composition with 50 km visibility (clear conditions) and 15 km visibility (slightly hazy conditions). In our band of interest, the α_{abs} can be approximated to a constant value resulting respectively around 0.95 and 0.91 (see Fig. 3).

In slightly hazy conditions, the aerosol extinction coefficient is almost constant up to 1 km. In clear conditions, the vertical distribution of aerosols is exponential. The α_{scatt} coefficient is given by Kruse-Kim model[18,19] as

$$\alpha_{\text{scatt}}(V,\lambda) = \frac{17}{V}\left(\frac{\lambda}{550}\right)^{-q(V)}, \tag{3}$$

where α_{scatt} is given in dB/km, V is the visibility in km, λ is the wavelength expressed in nm, and $q(V)$ is the particle size distribution,[16] which can be expressed by the Kim coefficient.[18] The total atmospheric loss due to absorption and scattering is estimated by

$$L_{atm} = \alpha_{abs}\sec(\theta) + \alpha_{scatt}L_{scatt}(\theta) \tag{4}$$

where $L_{scatt}(\theta)$ in km describes the slant range varying the elevation angle θ , α_{abs} is expressed in dB, α_{scatt} is expressed in dB/km

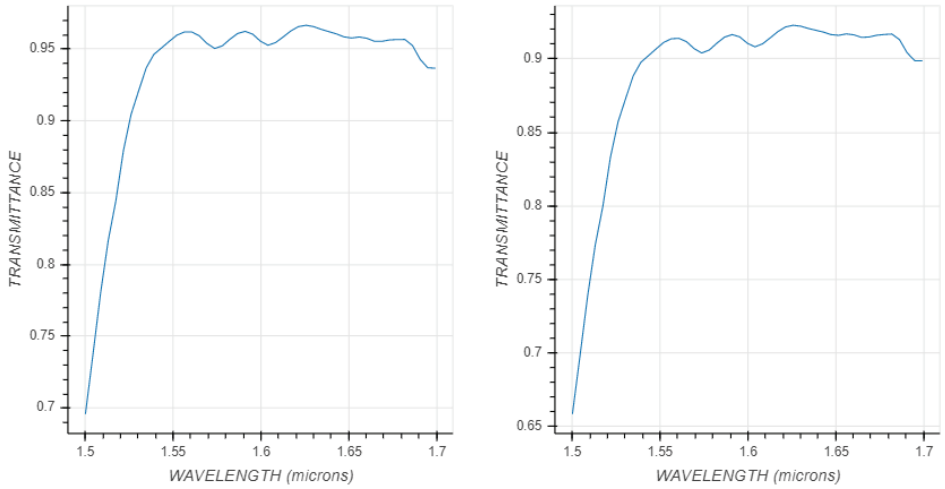

(a) (b)

Figure 3: Atmospheric transmittance in C-band in a Space-to-OGS path at 86° of elevation angle. A rural aerosol composition with a surface meteorological range, or visibility, of 50 km (clear conditions, on the left) and 15 km (slightly hazy conditions, on the right). The data refers to the case of an observer located at 2 km above sea level.

3.2 Scintillation

The effect of the atmospheric turbulence was characterized by the refractive index structure parameter $C_n^2(h)$. To describe this fluctuation strength along the vertical propagation path, we used the Hufnagel-Valley model, emended to include an OGS not located at sea level.[20]

$$\begin{aligned} C_n^2(h) = {} & 5.94 \times 10^{-53} \left(\frac{w_{rms}}{27}\right) h^{10} \exp(-h/1000) \\ & + 2.7 \times 10^{-16} \exp(-h/1500) + C_n^2(0) \exp(-h_0/700) \exp(-(h-h_0)/100) \end{aligned} \tag{5}$$

where w_{rms} is the root mean squared wind speed in [m/s] (pseudo-wind described in[12] following the Bufton wind profile), h is the satellite altitude [m], h_0 the OGS altitude [m] and $C_n^2(0)$ is the refractive index structure parameter at ground level in [$m^{-2/3}$].

From a communication point of view, the effect of the turbulence is a statistical fluctuation of the irradiance seen by the receiver, which can be modelled mathematically with a probability density function (pdf). In the last decades, different pdfs were proposed. The widely used ones are the log-normal distribution, which was demonstrated a reliably model in case of weak turbulence, and the Gamma-Gamma distribution, which could be used with a wider degree of generality.[12] In our work, thanks to the aperture averaging, which strongly reduces the value of Scintillation Index (SI), we used only the log-normal pdf.

Since atmospheric conditions can widely change, in our study, we considered two atmospheric and meteorological conditions, i.e. a favourable case, where the conditions pose very limited impairments, and a stressing case, where the propagation is highly affected. These two conditions are characterized by the parameters reported in Table 2. In these two cases, varying the elevation angle from the zenith to 30 deg we calculate the most relevant atmospheric parameters[12] (i.e., atmospheric Fried parameter r_0, Greenwood frequency f_G, Isoplanatic angle (IPA) θ_{IPA}, and Rytov scintillation index σ_R^2) in the two conditions. The results are reported in Table 3. As we can see, the most challenging link is for the "stressing atmospheric and meteorological conditions" at the lowest 30 degree elevation angle with an OGS at the sea level. In this scenario, the Rytov SI is quite high, causing a coherence diameter few centimeters.

A key parameter of the system is the size of the OGS telescope. Its immediate role is to determine the collected signal power, thus affecting the final OSNR at the pre-amplifier output. Furthermore, it can also

Table 2: Summary of atmospheric and meteorological conditions description.

ATMOSPHERIC CONDITIONS		
	Favourable atmospheric conditions	**Stressing atmospheric conditions**
Visibility [km]	50 (clear conditions)	15 (slightly hazy conditions)
Absorption coefficient	0.95 (clear conditions)	0.91 (slightly hazy conditions)
$C_n^2(0)$ $[m^{-2/3}]$	1.7×10^{-14}	1.7×10^{-13}
Wind speed at the ground level [m/s]	2	3

Table 3: Calculated atmospheric parameters based on atmospheric conditions defined in Table 2.

ATMOSPHERIC PARAMETERS				
	Favourable conditions		**Stressing conditions**	
	At 86° elevation	**At 30° elevation**	**At 86° elevation**	**At 30° elevation**
f_G at the sea level [Hz]	14.4	21.8	31.7	48
f_G at 2370 m [Hz]	11.4	17.2	14	21.3
r_0 at the sea level [cm]	19.3	12.7	5.6	3.7
r_0 at 2370 m [cm]	67.4	44.4	35.7	23.5
θ_{IPA} at the sea level [µrad]	26.2	8.7	25.6	8.5
θ_{IPA} at 2370 m [µrad]	35.0	11.5	35.3	11.6
σ_R^2 at the sea level	0.06	0.23	0.14	0.50
σ_R^2 at 2370 m	0.03	0.12	0.04	0.13

help reducing the impact of scintillation: as known, the irradiance at the receiver is a random variable, whose fluctuations are characterized by the SI. In our case, the receiver aperture of the OGS telescope is usually much larger than the atmospheric coherence diameter r_0.[12] Thus, the telescope collects several correlation patches partly compensating the effect of the fluctuations.

3.3 Pointing loss

As said, we did not consider in our model the PAT subsystem, which works before the link is established and during communication. However, once the two transceivers have locked onto each other, mechanical vibrations and noise in the tracking system can cause beam jitter or uncontrolled movements resulting in a residual pointing error θ_{point}.[14] This miss-pointing error is computed assuming a maximized transmitting antenna gain G_T with respect to pointing losses having a diffraction limited Gaussian beam in the paraxial case.[21,22] The residual transmitter pointing losses are modeled by[23]

$$L_{pointing} = e^{-\left(G_T \theta_{point}^2\right)} \tag{6}$$

where a Gaussian beam at the transmitter is assumed.

4. APERTURE AVERAGING AND AO SYSTEM

From the design point of view, it is known that we must equip the OGS with a sizable telescope and a performing system of AO, correcting a high number of Zernike modes.[24] Moreover, to further mitigate the atmospheric effects, the OGS should be sited at high altitude. Therefore, we introduce in our model these countermeasures, which are the key to detect the signal on the ground.

The aperture averaging effect becomes significant when the OGS telescope diameter is much greater than the minimum coherence diameter r_0, thus mitigating the intensity scintillation induced by the atmospheric

turbulence.[25] In Fig. 4, we report the computed SI in the strong turbulence conditions, for a point receiver (black dots) and for 1.2 m telescope, at OGS sited at 2370 m. As can be noted, the aperture averaging significantly reduces the value of the SI, strongly reducing the fluctuations at the receiver side.

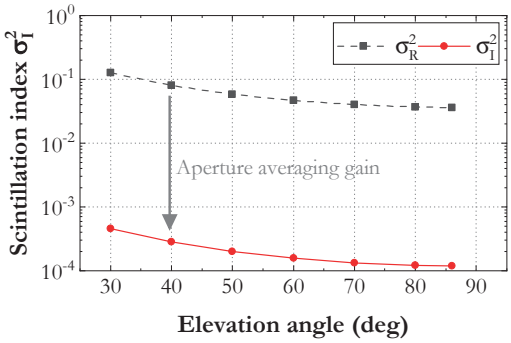

Figure 4: Effect of aperture averaging vs. elevation angle in the stressing condition, with a 250 mm GEO telescope: we report the SI for a point receiver (black dots) and for a 1.2 m wide telescope at 2370 m altitude (red dots).

When the ratio D/r_0 is greater than 1, the AO technique (partially) compensates for wavefront phase errors due to atmospheric turbulence, this is needed to increase the efficiency of the coupling of optical power from free-space to a single-mode fiber, which is the input to the pre-amplified WDM receiver. The modeled AO system is based on a Shack-Hartmann wavefront sensor (WFS), which measures the distortion on the downlink, a deformable mirror (DM) and a tip tilt mirror (TTM).[24,26–29] The performance are estimated according to.[24,26–29]

The reduction of scintillation and coupling efficiency are limited by the actual performance of the AO correction system. As example, in Fig. 5 we report the coupling loss values calculated as a function of the compensated Zernike modes, in the two cases of favourable and stressing conditions at 30° of elevation, in the case of a 1.2 m-wide telescope OGS at 2370 m altitude. As we see, the number of modes that we must be corrected is quite higher in the second case. In both cases, a good performance is obtained for at least 100 corrected modes. The two curves saturate at around -2.5 and -2.9 dB values, respectively, which are fully acceptable values.

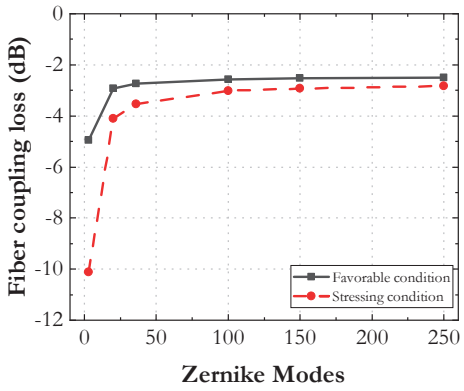

Figure 5: Effect of AO on fiber coupling: we report the coupling loss vs. the number of compensated Zernike modes, for the favourable condition (black solid curve) and the stressing condition (red dashed curve) at 30° of elevation, for a 1.2 m-wide telescope (red dots) at 2370 m altitude.

5. LINK BUDGET EVALUATION

Based on the previously defined atmospheric conditions, we investigated the system feasibility, by computing the link budget.

First, we started our analysis by considering a system configuration that is based on existing technologies. As an example, this is the case of telescope size, both on satellite and at OGS. Namely, in the following analysis, the system assumes the diameter of the GEO and OGS telescopes to be 135 mm and 1000 mm, respectively. Both telescopes have an obscuration factor of 0.3. We refer to this case as System-A: its detailed features are summarized in Table 4.

Table 4: Summary of initial system parameters for this study (System A).

PARAMETERS - SYSTEM A	
GEO telescope diameter [mm]	135
GEO telescope obscuration factor	0.3
Average residual pointing error [µrad]	4
OGS telescope diameter [mm]	1000
OGS telescope obscuration factor	0.3
Maximum booster optical power [dBm]	50

All channels are intensity-modulated at 40 Gbit/s. The system employs a FEC scheme for sensitivity improvement based on a RS(255,223). The AWG multiplexer has 100 GHz of channel spacing and 50 GHz 3 dB equivalent bandwidth on each optical port. The signals are then amplified by a single 50 dBm space qualified optical booster amplifying simultaneously all the optical WDM channels.[13] After free-space propagation, the signals are collected by the telescope, amplified by a EDFA (30 dB optical gain, 4 dB noise figure). Then the channels are demultiplexed by a similar AWG and each of them is detected by a conventional NRZ-OOK receiver. A summary of these parameters is presented in Table 5.

Table 5: Summary of WDM communication system parameters.

WDM COMMUNICATION SPECS	
Communication band	C (1530 nm to 1565 nm)
Number of wavelength channels	40
Data rate per channel [Gbit/s]	40
Modulation scheme	NRZ-OOK
FEC scheme	RS(255,223)
Required BER	10^{-9}
Channel Spacing [GHz]	100
AWG optical bandwidth [GHz]	50
Booster optical output power [dBm]	50
Pre-amplifier noise figure [dB]	4

After careful evaluation, we derive that this system configuration can not meet the requirements neither for favourable nor for stressing conditions. As we see in Table 6, in order to make the link work, the expected transmitter power should indeed exceed the limit of 50 dBm, which is already challenging. We note that free-space propagation is by far the most significant effect. Thus this is a clear indication that wider optics is needed both at transmitter and receiver size to increase the antenna gains.

We therefore studied the total link loss (including all propagation losses and telescope gains) as a function of the size of the transmitter (TX) and receiver (RX) telescopes. In all the following cases, we assume also that on

Table 6: Summary of link budget for System A. The link would be considered feasible if $P_{TX} \leq 50\,\mathrm{dBm}$, which is not found in any condition.

LINK BUDGET SYSTEM A				
Safety Margin [dB]	3			
GEO telescope Gain [dB]	106.5			
OGS telescope Gain [dB]	125.7			
Optical losses of the telescopes [dB]	-6			
Receiver sensitivity [dBm]	-37.3			
Atmospheric and meteo conditions	**Favourable conditions**		**Stressing conditions**	
Elevation angle [deg]	**86°**	**30°**	**86°**	**30°**
Link distance [km]	35.8×10^3	38.6×10^3	35.8×10^3	38.6×10^3
Free-space loss [dB]	-291.9	-292.6	-291.9	-292.6
Absorption and Scattering loss [dB]	-0.5	-1	-1.7	-3.5
Turbulence loss [dB]	-0.1	-0.1	-0.1	-0.1
Pointing error loss [dB]	-1.3	-1.3	-1.3	-1.3
Fiber coupling loss[dB]	-2.5	-2.4	-2.5	-2.8
Total required TX power [dBm]	53.2	54.5	54.6	57.3
Link feasibility	NO	NO	NO	NO

the satellite we can have available telescopes with no obscuration factor.[30] However, it is known that an OGS telescope without obscuration would be hard to be realized. Hence, we assumed that at OGS the telescope still has an obscuration of 30%.

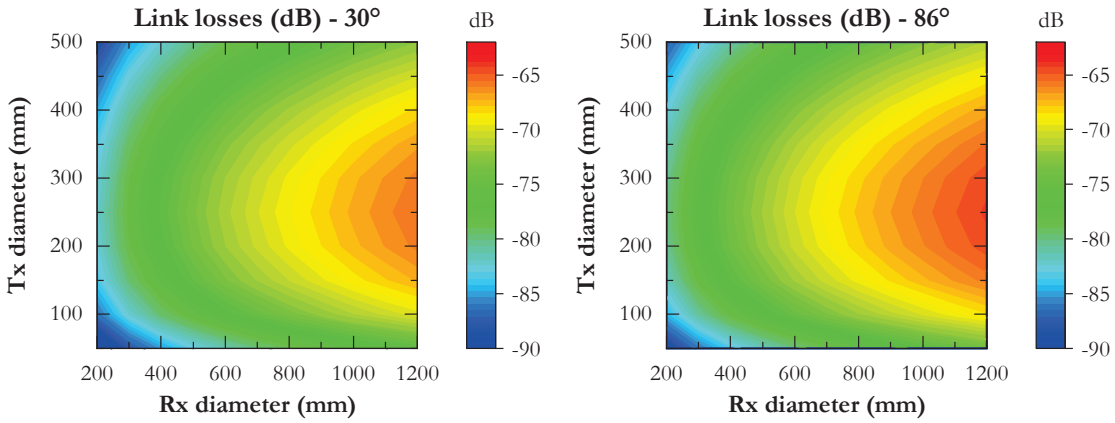

(a) (b)

Figure 6: Estimated total losses (in dB) at 2370 m altitude as function of GEO and OGS telescope diameters under favourable condition; elevation angle is 30 (a) and 86 (b) degrees.

We report in Fig. 6 the corresponding total losses at 2370 m altitude versus the diameter values of the TX and RX telescopes, for the favourable conditions, at elevation angles of 30 deg (left) and 86 deg (right). We spanned the GEO diameter from a minimum of 50 mm to 500 mm, with a step of 50 mm, and the OGS diameter from 200 mm to 1000 mm, with a step of 100 mm. The figures indicate the overall link losses, taking into account all the impairments and gains described in the previous sections. In the following Fig. 7, we present the data obtained, for the same elevation angles, in the stressing conditions. As expected, the optimal parameters are practically the same, although with higher total losses.

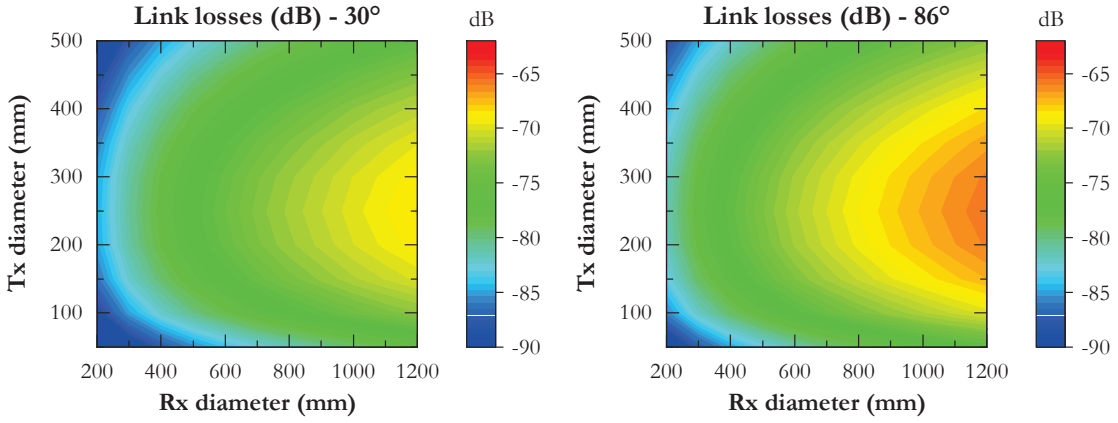

Figure 7: Estimated total losses (in dB) at 2370 m altitude as function of GEO and OGS telescope diameters under stressing condition; elevation angle is 30 (a) and 86 (b) degrees.

From these figures, we see a minimum on the link losses (red colored) with a GEO diameter of 250 mm and a OGS diameter of 1200 mm: we define this configuration as System B. Further increasing the transmitting telescope diameter leads to a steep increase of the pointing error, since the diffraction angle decreases, while reducing it, the diffraction angle increases, reducing the received optical power on the optical axis.

As can be seen, a small size of the receiving telescope clearly leads to a reduction of the collected light. Further increasing the size of the RX telescope, can still increase the collected light. This might be achieved, however, at expense of a worsening of AO performance, which strongly depend on the ratio D_r/r_0, in downlink. Therefore, an optimal TX diameter is found, at around 250 mm. On a satellite, this is a value that is not common, yet it seems quite feasible. A corresponding optimal value for the OGS could be expected from the above figures, but this value would exceed by far 1.2 m, which seems to be beyond the technology limits. Therefore, we did not consider having a telescope wider than 1.2 m. In conclusion, we included the two GEO and OGS telescope diameter values in the baseline for our further analyses. The results of this analysis are detailed in Table 7, which reports the technical features of System B. We note that, here, we are again assuming a maximum output power of 50 dBm. Actually, System B represents the best compromise solution to achieve the expected capacity in the considered link type.

In Fig. 8, we report the minimum required transmitted optical power to effectively close the link as a function of the elevation angle for both favourable and stressing conditions, in System B. As can be noted, the dependency on the elevation angle is limited, since the aperture averaging strongly reduces the scintillation index and therefore the dependency on the elevation angle, which usually has a strong impact. We note that the system needs more power in the stressing case, as expected. However, we estimate that it could work fine in all cases, provided that the maximum required optical power in the worst case is still 50 dBm, which is compatible with the new generation space-graded booster amplifier under development. However, the 30 degree case is actually borderline if we assume the stressing atmospheric conditions: in that case, the required power is exactly matching the 50 dBm value. This leaves no space for additional margins.

In order to conclude our analyses, in Table 8 we report the detailed link budget considering the System B. We note that, in the favourable conditions, around 47 dBm would be enough in all cases. This is achieved thanks to the fact that both telescopes are much wider than in System A, which overtakes the fact that the pointing error loss is a bit higher.

6. CONCLUSION

We have presented a complete numerical investigation of the feasibility of 1.6 Terabit/s feeder link (downlink). The assumed configuration is made of 40 Gbit/s OOK signals, with a RS FEC, in the C-band. The approach

Table 7: Summary of system parameters for this study.

PARAMETERS - SYSTEM B	
GEO telescope diameter [mm]	250
GEO telescope obscuration factor	0
Average residual pointing error [µrad]	4
OGS telescope diameter [mm]	1200
OGS telescope obscuration factor	0.3
Maximum booster optical power [dBm]	50

Table 8: Summary of link budget analysis: System B. The link is considered feasible if $P_{TX} \leq 50\,\text{dBm}$.

LINK BUDGET SYSTEM B				
Safety Margin [dB]	3			
GEO telescope Gain [dB]	113.2			
OGS telescope Gain [dB]	127.3			
Optical losses of the telescopes [dB]	-6			
Receiver sensitivity [dBm]	-37.3			
Atmospheric and meteo conditions	**Favourable conditions**		**Stressing conditions**	
Elevation angle [deg]	**86°**	**30°**	**86°**	**30°**
Link distance [km]	35.8×10^3	38.6×10^3	35.8×10^3	38.6×10^3
Free-space loss[dB]	-291.4	-292.0	-291.4	-292.0
Absorption and Scattering loss [dB]	-0.5	-1	-1.7	-3.5
Turbulence loss [dB]	-0.1	-0.1	-0.1	-0.1
Pointing error loss [dB]	-4.4	-4.4	-4.4	-4.4
Fiber coupling loss [dB]	-2.4	-2.5	-2.5	-2.9
Total required TX power [dBm]	45.9	47.3	47.3	50.0
Link feasibility	YES	YES	YES	YES

strongly relies upon the assumption that current photonic components can be used on a GEO-satellite and that a high power booster amplifier ($\leq 50\,\text{dBm}$ output power) and optimized optics can be deployed. We considered two scenarios of atmospheric conditions, i.e. a favourable and a stressing case.

Indeed, we found that the best (realistic) operating conditions are an un-obscurated 25 cm-wide GEO transmitter telescope and a 1.2 m-wide OGS receiver telescope sited at 2370 m altitude. These two values are achievable with existing technology, although quite challenging. They also require suitable AO system, able to correct the wavefront distortions due to turbulence effect, thus increasing the overall detected power. In the considered different atmospheric conditions, we found that, in both cases, the system can be designed to operate, although with higher TX power in the stressing condition.

Finally, we note that we did not include other modulation formats (e.g. DPSK) neither coherent detection. We expect, however, that, in the link budget, the benefits of these solutions may be on the order of few dB's (considering that the system is OSNR-limited anyway). This would allow a reduction of the total output power, but the optics would likely stay untouched.

The present design indicates specifications of the system that are not far from those of existing elements. In particular, optical terminals with 135 mm diameter at GEO are already in place on satellites; they may be upgraded to a wider size. At OGS, we recall that a 1 m ESA telescope is already installed in the Teide Observatory in the Canary Islands (Spain) at 2370 m above the sea level. Not by chance, this altitude value is what we assumed in our calculations. Lower values would result in higher impairments.

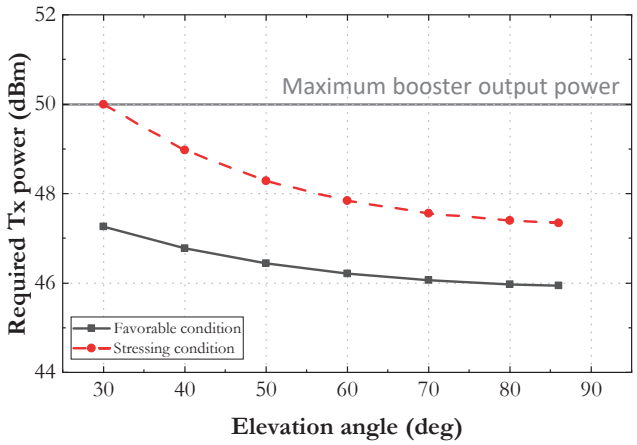

Figure 8: Minimum required transmitted optical power for System B.

On the other hand, photonic devices and subsystems compatible with our WDM design can benefit from a strong heritage from optical fiber communications, but they still have to be space-qualified. Probably, among the various building blocks, the most challenging technology is the high-power booster, which should be developed and space-qualified. Although space-qualified 40 dBm amplifiers exist, 50 dBm are very challenging. Finally, PAT and AO blocks should also be refined to meet the system requirements. These results can be used as first guidelines for FSOC system designers of future links.

ACKNOWLEDGMENTS

This work was supported in part by the European Space Agency under the project HydRON - Phase A (High Throughput Optical Network)

REFERENCES

[1] Kodheli, O., Lagunas, E., Maturo, N., Sharma, S. K., Shankar, B., Montoya, J. F. M., Duncan, J. C. M., Spano, D., Chatzinotas, S., Kisseleff, S., Querol, J., Lei, L., Vu, T. X., and Goussetis, G., "Satellite communications in the new space era: A survey and future challenges," *IEEE Communications Surveys & Tutorials* **23**(1), 70–109 (2021).

[2] Cowley, W., Giggenbach, D., and Calvo, R. M., "Optical transmission schemes for geo feeder links," (2014).

[3] Robinson, B. S., Boroson, D. M., Schieler, C. M., Khatri, F. I., Guldner, O., Constantine, S., Shih, T., Burnside, J. W., Hakimi, F. Q., Bilyeu, B. C., Garg, A., Allen, G., Clements, E., and Cornwell, D. M., "Terabyte infrared delivery (tbird): a demonstration of large-volume direct-to-earth data transfer from low-earth orbit," (2018).

[4] Hauschildt, H., Elia, C., Moeller, H. L., El-Dali, W., Navarro, T., Guta, M., Mezzasoma, S., and Perdigues, J., "Hydron: High throughput optical network," *2019 IEEE International Conference on Space Optical Systems and Applications (ICSOS)* , 1–6, IEEE, Portland, OR, USA (2019).

[5] Hauschildt, H., Elia, C., Moeller, H. L., El-Dali, W., Navarro, T., Guta, M., Mezzasoma, S., and Perdigues, J., "Hydron: High throughput optical network," in [*Free-Space Laser Communications XXXII*], *Society of Photo-Optical Instrumentation Engineers (SPIE) Conference Series* **11272**, 112720B (Mar. 2020).

[6] Satoh, Y., Miyamoto, Y., Takano, Y., Yamakawa, S., and Kohata, H., "Current status of Japanese optical data relay system (JDRS)," *2017 IEEE International Conference on Space Optical Systems and Applications (ICSOS)* , 240–242 (2017).

[7] Yadav, A., Agarwal, M., Agarwal, S., and Verma, S., "Internet from space anywhere and anytime - starlink," *SSRN Electronic Journal* (01 2022).

[8] Spring-Turner, C. and Rajan, R., "Performance bounds for cooperative localisation in the starlink network," (07 2022). arXiv.

[9] Consultative Committee for SpaceData Systems (CCSDS), "Orange book, issue 1," (Dec. 2018).

[10] Mata-Calvo, R., Calia, D. B., Barrios, R., Centrone, M., Giggenbach, D., Lombardi, G., Becker, P., and Zayer, I., "Laser guide stars for optical free-space communications," in [*Free-Space Laser Communication and Atmospheric Propagation XXIX*], Hemmati, H. and Boroson, D. M., eds., **10096**, 100960R, International Society for Optics and Photonics, SPIE (2017).

[11] Sodnik, Z., Voland, C., Perdigues, J., Fischer, E., Kudielka, K., and Czichy, R., "Optical feeder-link between ESA's optical ground station and Alphasat," in [*International Conference on Space Optics — ICSO 2020*], **11852**, 1185218, International Society for Optics and Photonics, SPIE (2021).

[12] Andrews, L. C. and Phillips, R. L., [*Laser beam propagation through random media*], SPIE Optical Engineering Press (2005).

[13] ITT European Space Agency, "WDM high power optical amplifier at 1550 nm," (Mar. 2021). https://esastar-publication-ext.sso.esa.int/ESATenderActions/details/6954.

[14] Arnon, S., Rotman, S., and Kopeika, N. S., "Beam width and transmitter power adaptive to tracking system performance for free-space optical communication," *Appl. Opt.* **36**, 6095–6101 (Aug 1997).

[15] Anderson, D., McGookin, M., and Brignall, N., "Fast model predictive control of the nadir singularity in electro-optic systems," *Journal of Guidance Control and Dynamics - J GUID CONTROL DYNAM* **32**, 626–632 (03 2009).

[16] Prokes, A., Wilfert, O., and Petrzela, J., "Comparison of atmospheric losses in 850 nm and 1550 nm optical windows," in [*2010 IEEE Region 8 International Conference on Computational Technologies in Electrical and Electronics Engineering (SIBIRCON)*], 310–313 (2010).

[17] Weichel, H., [*Laser beam propagation in the atmosphere*], vol. 10319, SPIE press (1990).

[18] Kim, I. I., McArthur, B., and Korevaar, E. J., "Comparison of laser beam propagation at 785 nm and 1550 nm in fog and haze for optical wireless communications," (feb 2001).

[19] Fredericks, W. J., "Elements of infrared technology. generation, transmission, and detection. paul w. kruse, laurence d. mcglauchlin, and richmond b. mcquistan. wiley, new york, 1962. xxi + 448 pp. illus. $10.75," **137**, 123–123 (1962).

[20] Dimitrov, S., Matuz, B., Liva, G., Barrios, R., Mata-Calvo, R., and Giggenbach, D., "Digital modulation and coding for satellite optical feeder links," in [*2014 7th Advanced Satellite Multimedia Systems Conference and the 13th Signal Processing for Space Communications Workshop (ASMS/SPSC)*], 150–157 (2014).

[21] Valentini, L., Faedi, A., Paolini, E., and Chiani, M., "Analysis of pointing loss effects in deep space optical links," in [*2021 IEEE Global Communications Conference (GLOBECOM)*], 1–6, IEEE Press (2021).

[22] Marshall, W. K., "Transmitter pointing loss calculation for free-space optical communications link analyses," *Appl. Opt.* **26**, 2055–2057 (Jun 1987).

[23] Chen, C.-C. and Gardner, C., "Impact of random pointing and tracking errors on the design of coherent and incoherent optical intersatellite communication links," *IEEE Transactions on Communications* **37**(3), 252–260 (1989).

[24] Fedrigo, E., Kasper, M., Ivanescu, L., and Bonnet, H., "Real-time control of eso adaptive optics systems (echtzeitsteuerung der eso adaptive optik systeme)," **53**(10), 470–483 (2005).

[25] Fried, D. L., "Statistics of a geometric representation of wavefront distortion," *J. Opt. Soc. Am.* **55**, 1427–1435 (Nov 1965).

[26] Wang, Y., Xu, H., Li, D., Wang, R., Jin, C., Yin, X., Gao, S., Mu, Q., Xuan, L., and Cao, Z., "Performance analysis of an adaptive optics system for free-space optics communication through atmospheric turbulence," *Scientific Reports* **8** (2018).

[27] Amjad, A., Zhang, C., Mohsan, S. A. H., Lyu, W., Amjad, R., Chen, X., and Xu, J., "Underwater wireless-to-plastic optical fiber communication systems with a passive front end," 1–3 (08 2019).

[28] Hardy, J. W., [*Adaptive optics for astronomical telescopes Vol.16*], Oxford series in optical and imaging sciences, Oxford University Press (1998).

[29] Tyson, R. K., "Adaptive optics and ground-to-space laser communications," *Appl. Opt.* **35**, 3640–3646 (Jul 1996).

[30] Drège, E. M., Skinner, N. G., and Byrne, D. M., "Analytical far-field divergence angle of a truncated gaussian beam," *Appl. Opt.* **39**, 4918–4925 (Sep 2000).